

## Supporting Information

# Photo-Responsive Self-Reducible Polymers: Overcoming the Spatiotemporal Barriers for Hypersensitivity

Chuang Weng, Haodong Chen, Taoran Xu, Zifen Li, Xinfu Liu, Mingming Ding\*, Qin Zhang,  
Hong Tan, Qiang Fu\*

<sup>a</sup> *College of Polymer Science and Engineering, State Key Laboratory of Polymer Materials Engineering,  
Sichuan University, Chengdu 610065, China*

### Materials and Method

**Materials.** Triphosgene (99%) was purchased from Adams Reagent Co., Ltd. (Shanghai, China). Dimethyl L-cystinate dihydrochloride (Cys·OMe·2HCl, 98%) was obtained from Shanghai Haohong Huagong Technology Co., Ltd. (Shanghai, China). Dithiothreitol (DTT, 99%) was purchased from Inalco Spa (Milano, Italy). *o*-Nitrobenzyl bromide (ONB) was attained from Accela ChemBio Co., Ltd. (Shanghai, China). Methoxyl-poly (ethylene glycol) (MPEG, MW2000, 99%) and 3,3'-Diethylthiadicarbocyanine iodide (Cy5) were purchased from Alfa Aesar (China)

Chemistry Co., Ltd. (Shanghai, China). Nile red (NR) and rhodamine 6G (R6G, 95%) were purchased from TCI Development Co., Ltd. (Tokyo, Japan). Doxorubicin hydrochloride (DOX·HCl) was obtained from Meilun Biotechnology Co., Ltd. (Dalian, China). Pyridine (AR) was attained from Li Anlong Bohua Pharmaceutical Chemical Co., Ltd. (Tianjin, China). Thioflavin T (ThT) was purchased from Acros Organics (New Jersey, USA). Dichloromethane (DCM, AR), sodium hydroxide (AR), diethyl ether (AR), *n*-hexane (AR) and dimethyl sulfoxide (DMSO, AR) were provided by Chengdu KeLong chemical reagent factory (Sichuan, China). Ethyl alcohol and triethylamine (TEA, AR) were purchased from Chengdu Changlian Chemical Reagent Co., Ltd. (Sichuan, China). Tetrahydrofuran (THF) was obtained from Shanghai Titan Scientific Co., Ltd. (Shanghai, China), and reflux distilled with sodium filament and benzophenone under nitrogen condition.

### **Characterization**

Nuclear magnetic resonance spectroscopy ( $^1\text{H}$  NMR, 400 MHz) was recorded on a Bruker Avance III HD 400MHz spectrometer at room temperature using DMSO- $d_6$  as solvents and tetramethylsilane (TMS) as an internal standard.

Fourier transform infrared (FTIR) spectroscopy was collected on a Nicolet iS10 spectrometer (Thermo Electron Corporation, U.S.A) from 4000 to 500  $\text{cm}^{-1}$ .

Mass spectrometry (MS) was tested using an HP100-LC/MSD mass spectrometer with electrospray ionization (ESI) mode.

Gel permeation chromatography (GPC) was carried out using a Waters-1515 (USA) gel permeation chromatograph with a mobile phase of THF at a flow rate of 1 mL min<sup>-1</sup>.

Differential scanning calorimetry (DSC) were performed on a DSC8000 (USA) at a scanning speed of 10 °C min<sup>-1</sup> over a temperature range of 0-100 °C. Ultrahigh pure nitrogen was used as the pure gas at a flow rate of 20 mL min<sup>-1</sup>.

The X-ray diffraction (XRD) patterns were acquired on a Philips X' Pert PRO, XL-30 diffractometer with Cu4K $\alpha$  radiation. The XRD data over the 5-60° range were collected.

Circular dichroism (CD) was measured on a J-1500-150 spectrometer (JASCO Corporation, Japan) at room temperature in the range of 190 nm to 270 nm. The sample solution was placed using a quartz cell containing a 1 mm optical path. The average residual molar ellipticity of polymers based on apparent ellipticity was calculated using the following formula: ellipticity ( $[\theta]$  in deg cm<sup>2</sup> dmol<sup>-1</sup>) = (millidegrees  $\times$  mean residue weight)/ (path length in millimeters  $\times$  concentrations of polypeptide in mg mL<sup>-1</sup>).<sup>1</sup>

Static light scattering (SLS) and dynamic light scattering (DLS) experiments were performed on a Brookhaven Instrument (Brookhaven Instruments Corporation) equipped with a BI-200SM goniometer, a BI-9000 correlator and a solid-state laser emitting at 532 nm. The samples were prepared from aqueous polymer solutions and kept at 25 °C during measurements. The detection angles ranged from 30° to 150°. Three repeat measurements of scattered light intensity were taken at each angle and concentration. CONTIN analyses were used for the extraction of  $R_H$  data from DLS

measurements. The  $R_G$  data were estimated by the angular dependence of the scattering intensity from SLS measurements. Finally, the characteristic parameter ( $\rho$ ) was calculated from the ratio of  $R_G / R_H$ .<sup>2-4</sup>

Transmission electron microscopy (TEM) was observed on a Hitachi model H-600-4 transmission electron microscope. In brief, 1-2 drops of sample liquid were dropped onto a Formvar film coated copper mesh and stained with 1% (w/v) phosphotungstic acid, and excess liquid was removed by filter paper and dried. The morphology was then observed at an acceleration voltage of 75 kV.

Small-angle X-ray scattering (SAXS) experiment was conducted on an Xeuss 2.0 instrument (Xenocs Corporation, France). A Dectris Pilatus detector and Cu-K  $\alpha$  radiation ( $\lambda = 1.54 \text{ \AA}$ ) were used under a vacuum at room temperature to test the polymer aqueous dispersion ( $10 \text{ mg mL}^{-1}$ ) packed in a quartz capillary ( $d = 1.5 \text{ mm}$ ). Data was collected using a Dectris Pilatus detector with a distance of 2.5 m between the sample and the detector and an exposure time of 30 min. All the samples were analyzed in the  $q$  range of 0.01 to  $1 \text{ \AA}^{-1}$ , and the length of scattering vector  $q$  was defined as:

$$\begin{aligned} q &= (4\pi\sin\theta) / \lambda \\ &= 2\pi / d \end{aligned}$$

where  $\lambda$  is the wavelength of the X-ray, and  $\theta$  is half of the scattering angle. The SAXS data were reduced to remove the solvent background from the acquired sample scattering profiles using a Foxtrot 3.2.7 software, and further analyzed by fitting to model expressions using a SasView 5.0 software package.<sup>5-7</sup> The SAXS data of PRSRP

can be reasonably fitted by a vesicle model (Figure S9), in agreement with TEM, DLS/SLS, R6G encapsulation and CLSM measurements. It should be noted that the scattering signal was relatively weak and imperfect with some deviation of the SAXS data at high scattering vectors, possibly because of the wide size distribution and low concentration of the samples.<sup>8-11</sup> To better understand the self-assembly behavior of PRSRP, further synchrotron SAXS and small-angle neutron scattering (SANS) with high resolution scattering patterns will be performed in our future work.<sup>12-18</sup>

UV-Vis spectra were collected using a UV2600 spectrophotometer (Techcomp, Ltd., China) in the wavelength range of 200-800 nm.

Fluorescence measurement was conducted on an F-4600 FL spectrophotometer (Hitachi, Ltd., Japan). For R6G fluorescence, the emission spectra were collected from 530 nm to 800 nm at  $\lambda_{\text{ex}}$  of 526 nm. For NR fluorescence, the emission spectra were collected from 540 nm to 800 nm at  $\lambda_{\text{ex}}$  of 520 nm. For DOX fluorescence, the emission spectra were collected from 500 nm to 800 nm at  $\lambda_{\text{ex}}$  of 480 nm.

### **Synthesis of *o*-Nitrobenzyl-Caged Dithiothreitol (ONB-DTT, 1)**

DTT (3.08 g, 20 mM) was dissolved in 40 mL ethanol solution containing 1 M NaOH and cooled in an ice bath. Then 10.37 g (48 mM) of ONB in ethanol (40 mL) was added dropwise, and the reaction was performed at room temperature for 5 h. The white solid product was filtered, washed with ethanol, freeze-dried and stored in the dark (63.3% yield).

$^1\text{H}$  NMR (400 MHz,  $\text{CDCl}_3$ , TMS,  $\delta$  in ppm): 7.98 (dd, 1H,  $-\text{C}=\text{CH}$ ), 7.50 (dd, 1H,  $-\text{C}=\text{CH}$ ), 4.11 (q, 2H,  $\text{CH}_2\text{-S-}$ ), 3.75 (m, 2H,  $-\text{CH}_2\text{-O}$ ), 2.80 (s, 2H,  $-\text{CH}_2\text{-}$ ).  $^{13}\text{C}$  NMR (400 MHz,  $\text{DMSO-}d_6$ ,  $\delta$ ): 148.17, 133.91, 132.96, 131.68, 128.57, 125.37, 72.83, 35.58, 33.37. FTIR ( $\text{cm}^{-1}$ ): 3334 (m,  $\nu$  O-H ), 3047 (s,  $\nu$  C-H ), 1600 (s,  $\nu$  C=C), 1560 (m,  $\nu_{\text{as}}$   $\text{NO}_2$ ), 1450 (s,  $\nu$  C-C), 710, (w,  $\nu$  C-S). MS (ESI, positive)  $m/z$ : Calcd, 447.0655; found, 447.0633.

### Synthesis of L-Cystine Dimethyl Ester Diisocyanate (CDI, 2)

Cys·OMe·2HCl (10.2 g, 30 mM) was dissolved in anhydrous DCM and pyridine under dry argon. Then triphosgene (7.7 g, 26 mM) was dissolved in DCM and added dropwise into the reaction system for 5 h of reaction at  $-5^\circ\text{C}$ . Afterward, the reaction mixture was washed with cold HCl solution (0.5 M) and deionized water for three times. The organic phase was collected and dried with anhydrous  $\text{Na}_2\text{SO}_4$  overnight. Then the solution was filtered and condensed under reduced pressure. The crude products were purified by recrystallization from dried THF/*n*-hexane to obtain a white needle-shaped solid (75.0 % yield).

$^1\text{H}$  NMR (400 MHz,  $\text{CDCl}_3$ , TMS,  $\delta$  in ppm): 4.40 (dd, 1H,  $=\text{N-CH}$ ), 3.85 (s, 3H,  $-\text{O-CH}_3$ ), 3.21 (dd, 1H,  $-\text{S-CH}_2$ ), 3.07 (dd, 1H,  $-\text{S-CH}_2$ ).  $^{13}\text{C}$  NMR (400 MHz,  $\text{CDCl}_3$ ,  $\delta$ ): 169.6, 127.56, 56.58, 53.63, 42.97. FTIR ( $\text{cm}^{-1}$ ): 2260(s,  $\nu$   $\text{N}=\text{C}=\text{O}$ ), 1750 (s,  $\nu$   $\text{C}=\text{O}$ ), 1300 (s,  $\nu$  C-O-C). MS (ESI, positive)  $m/z$ : Calcd, 320.0137; found, 320.0183.

### Synthesis of Photo-Responsive Self-Reducible Polymer (PRSRP, 3)

PRSRP was synthesized by a facile one-pot solution polymerization. By changing the feed ratios of monomers, the molecular weights of polymers could be well controlled. In brief, ONB-DTT (0.85 / 1.7 g) and CDI (1.01 / 1.68 g) were dissolved in anhydrous THF (15 mL) in a flask. Then stannous octoate (0.1%) was added, and the reaction was carried out at 60 °C for 12 h under argon atmosphere. Afterward, pre-dehydrated MPEG (4 g) was added into the system, and the reaction was continued for 24 h. The solution was precipitated in ice diethyl ether for three times to obtain a white solid (78.4% yield).

### Synthesis of Photo-Responsive Irreducible Polymer (PRIRP)

PRIRP was synthesized according to Scheme S1 by a facile one-pot solution polymerization. In brief, ONB-DTT (1.69 g) and LDI (1.19 g) were dissolved in anhydrous tetrahydrofuran (THF) (15 mL) in a flask. Then stannous octoate (0.1%) was added, and the reaction was carried out at 60 °C for 12 h under argon atmosphere. Afterward, pre-dehydrated MPEG (4 g) was added into the system, and the reaction was continued for 24 h. The solution was precipitated in ice diethyl ether for three times to obtain a white solid (81.4% yield).

The structure of PRIRP was confirmed by  $^1\text{H}$  NMR, FTIR and GPC. As could be seen from the  $^1\text{H}$  NMR spectra (Figure S16), The peaks at 7.89 ( $=\text{CH}-\text{C}-\text{NO}_2$ ), 7.80 ( $-\text{CH}=\text{CH}-\text{C}-\text{NO}_2$ ), 7.51( $=\text{CH}-\text{C}$ ) and 4.33 ( $-\text{CH}_2-\text{S}$ ) ppm are assigned to the benzene ring in ONB. The peak at 5.02 ppm ( $-\text{CH}_2\text{O}-$ ) is ascribed to DTT. The peaks corresponding to the methylene and methyl groups in LDI residue were found at 3.40 ( $-\text{CH}_2\text{CH}_2-\text{NH}-$ ) and 1.61 ppm ( $\text{CH}_3-\text{CH}_2-$ ), respectively. The peak at 3.6 ppm ( $-\text{CH}_2\text{CH}_2-\text{NH}-$ ) and 1.61 ppm ( $\text{CH}_3-\text{CH}_2-$ ), respectively. The peak at 3.6 ppm ( $-\text{CH}_2\text{CH}_2-\text{NH}-$ ) and 1.61 ppm ( $\text{CH}_3-\text{CH}_2-$ ), respectively.

$\text{CH}_2\text{CH}_2\text{O}-$ ) is ascribed to the methylene groups of PEG block.

The FTIR spectra of PRIRP are depicted in Figure S17. The characteristic peak of  $-\text{N}=\text{C}=\text{O}$  group ( $2270\text{ cm}^{-1}$ ) disappears, indicating that the isocyanate groups in LDI have been completely reacted with ONB-DTT and MPEG. At the same time, the obvious peaks can be seen at  $3300\text{--}3500\text{ cm}^{-1}$ , mainly due to the N-H stretching vibration. The stretching bands observed at  $1600\text{--}1800\text{ cm}^{-1}$  region correspond to  $\text{C}=\text{O}$  stretching in ester and urethane groups. The characteristic peak at  $1650\text{--}1600\text{ cm}^{-1}$  is ascribed to the benzene ring carbon skeleton in ONB-DTT. The antisymmetric and symmetric stretching vibration of nitro were found at  $1600\text{--}1450\text{ cm}^{-1}$  and  $1350\text{--}1300\text{ cm}^{-1}$ , respectively. The peak at  $1113\text{ cm}^{-1}$  can be attributed to the C-O vibration peak in PEG. GPC diagrams indicates that the number average molecular weight of PRIRP is  $12483\text{ g mol}^{-1}$  with a narrow molecular weight distribution, which is similar to that of PRSRP. The results confirm that the control polymer PRIRP has been successfully synthesized.

### **Preparation of Polymeric Assemblies**

The self-assembly of PRSRP and PRIRP was performed by a dialysis method. Briefly, a solution of polymers (10 mg) in 1 mL of THF was added dropwise to 9 mL of deionized water with rapid stirring. The solution was transferred to a dialysis bag (MWCO 3500), and dialyzed against deionized water for 3 d, replacing the external water once 3 h. Finally, the solution was centrifuged at  $3000\text{ r min}^{-1}$  for 15 min and filtered through a  $0.45\text{ }\mu\text{m}$  pore-sized syringe filter (Millipore, Carrigtwohill, Co. Cork, Ireland).



### **Encapsulation of R6G Probe**

0.2 mL of an aqueous solution of rhodamine 6G (R6G) ( $0.2 \text{ mg mL}^{-1}$ ) was added dropwise into 2 mL of polymeric assemblies ( $0.2 \text{ mg mL}^{-1}$ ). The solution was ultrasonicated at 40-50 °C for 2 h in the dark and dialyzed against deionized water for 24 h (MWCO 3500) to remove free R6G. Free R6G dissolved in an aqueous solution was used as a control, with the R6G concentration in water was adjusted so that the UV-Vis absorption matched the intensity of R6G encapsulated in vesicles (Figure S9). The fluorescence emission spectra of R6G in water and assembled solutions were recorded on an F-4600 FL spectrophotometer (Hitachi, Ltd., Japan). The excitation wavelength was 526 nm and the slit width was 10.0 nm.

### **Encapsulation of DOX·HCl and FITC Probes**

To provide more direct evidence for the vesicular structure, a solution of DOX·HCl in water ( $150 \text{ }\mu\text{L}$ ,  $0.05 \text{ mg mL}^{-1}$ ) was added dropwise into 1 mL of PRSRP assemblies ( $2 \text{ mg mL}^{-1}$ ). Afterward, the solution was stirred for 0.5 h. After extensive dialysis (MWCO 3500) for 12 h to remove free DOX·HCl,  $150 \text{ }\mu\text{L}$  of FITC in acetone ( $0.05 \text{ mg mL}^{-1}$ ) was added drop-wise into the solutions. Free dyes and acetone were then removed by dialysis (MWCO 3500) against water, centrifugalized at  $3000 \text{ r min}^{-1}$  for 10 min and passed through a 0.45 mm pore-sized syringe filter (Millipore, Carrigtwohill, Co. Cork, Ireland). The resulting fluorescent-encapsulated assemblies were dropped on a glass slide, air-dried and mounted with 10% glycerol solution, then imaged by a confocal laser scanning microscope (CLSM, Olympus FV1000, Japan) with an objective of 100× magnification and 1.49 NA.

## Thioflavin T (ThT) Binding Assay

ThT binding assay was used to investigate the unique layered structure of PRSRP assemblies. In brief, ThT was added into polymer solution to a final ThT concentration of 20  $\mu\text{M}$ . The fluorescence emission spectra were recorded from 450 to 600 nm on an F-4600 FL spectrophotometer (Hitachi, Ltd., Japan). The excitation wavelength was 440 nm, and the slit width was set to 5 nm.

## Computational Simulation

The vesicle structure of the PRSRP was simulated using a dissipative particle dynamics (DPD) method. DPD is a relatively new method proposed to study the behavior of complex fluids.<sup>19-21</sup>

$$\frac{d\mathbf{r}_i}{dt} = \mathbf{v}_i \quad (1)$$

and

$$m_i \frac{d\mathbf{v}_i}{dt} = \mathbf{f}_i \quad (2)$$

where  $\mathbf{r}_i$ ,  $\mathbf{v}_i$ ,  $m_i$  and  $\mathbf{f}_i$  are the position, velocity, mass of the  $i$ th particle, and the total forces acting on particle  $i$ , respectively. The force is composed of three different pairwise-additive forces: conservative ( $\mathbf{F}^C$ ), dissipative ( $\mathbf{F}^D$ ), random forces ( $\mathbf{F}^R$ ). The interaction between two particles can be written as the sum of these forces,<sup>22</sup>

$$\mathbf{f}_i = \sum_{j \neq i} (\mathbf{F}_{ij}^C + \mathbf{F}_{ij}^D + \mathbf{F}_{ij}^R) \quad (3)$$

The conservative force  $\mathbf{F}_{ij}^C$  is a soft repulsion acting along the line of the centers and is given by

$$\mathbf{F}_{ij}^C = \begin{cases} -\alpha_{ij}(r_c - r_{ij}) \mathbf{n}_{ij}, & r_{ij} < r_c \\ 0, & r_{ij} \geq r_c \end{cases} \quad (4)$$

where  $a_{ij}$  is a maximum repulsion force between particles  $i$  and  $j$ ,  $\mathbf{r}_{ij}$  is the vector from position  $i$  to  $j$ ,  $\mathbf{r}_{ij} = \mathbf{r}_j - \mathbf{r}_i$ ,  $r_{ij} = |\mathbf{r}_{ij}|$ ,  $\mathbf{n}_{ij} = \mathbf{r}_{ij} / |\mathbf{r}_{ij}|$  and cutoff radius  $r_c$ . The repulsion parameters between particles of different types correspond to the mutual solubility, expressed as the Flory–Huggins  $\chi$ -parameter. The relation is as follows:

$$a_{ij} \approx a_{ii} + 3.27\chi_{ij} \quad (5)$$

The dissipative force is a friction force that reduces the velocity differences between DPD beads, which is given by

$$\mathbf{F}_{ij}^D = \begin{cases} -\gamma\omega^D(r_{ij})(\mathbf{n}_{ij} \cdot \mathbf{v}_{ij})\mathbf{n}_{ij}, & r_{ij} < r_c \\ 0, & r_{ij} \geq r_c \end{cases} \quad (6)$$

Where  $\gamma$  is a friction parameter,  $\omega^D(r_{ij})$  is the weighting function, and  $\mathbf{v}_{ij} = \mathbf{v}_j - \mathbf{v}_i$ . The form is chosen to conserve the total momentum of each pair of particles and therefore the total momentum of the system is conserved. The dissipative force acts to reduce the relative momentum between particles  $i$  and  $j$ , while random force is to impel energy into the system. The random force also acts between all pairs of particles as

$$\mathbf{F}_{ij}^R = \begin{cases} \sigma\omega^R(r_{ij})\xi_{ij}\Delta t^{-1/2}\mathbf{n}_{ij}, & r_{ij} < r_c \\ 0, & r_{ij} \geq r_c \end{cases} \quad (7)$$

The randomness is contained in the element  $\xi_{ij}$ , which is a randomly fluctuating variable with Gaussian statistics,

$$\langle \xi_{ij}(t) \rangle = 0 \quad (8)$$

and

$$\langle \xi_{ij}(t)\xi_{kl}(t') \rangle = (\delta_{ik}\delta_{jl} + \delta_{il}\delta_{jk})\delta(t - t') \quad (9)$$

They are assumed to be uncorrelated for different pairs of particles and time. There is a relation between the two weighting functions and two parameters,

$$\omega^D(r_{ij}) = [\omega^R(r_{ij})]^2 \quad (10)$$

and

$$\sigma^2 = 2\gamma kT, \quad (11)$$

we choose the weighting functions as follows:

$$\omega^D(r_{ij}) = [\omega^R(r_{ij})]^2 = \begin{cases} (r_c - r_{ij})^2, & r_{ij} < r_c \\ 0, & r_{ij} \geq r_c \end{cases} \quad (12)$$

In our study, we consider an aqueous solution ( $W$ ) of photo-responsive self-reducible polymer (PRSRP). The PRSRP is molded as  $E_x(CO)_yE_x$ , where  $E$ ,  $C$  and  $O$  represent PEG segments, CDI residues and DTT-ONB groups, respectively. The interaction parameters are chosen in an attempt to retain the characteristic interactions associated with  $E$ ,  $C$  and  $O$  beads. According to previous reports, the repulsive parameter between two alike particles is set to  $\alpha_{ij} = 25.0$  ( $\alpha_{WW}$ ,  $\alpha_{EE}$ ,  $\alpha_{CC}$ ,  $\alpha_{OO}$ ) to reflect the correct compressibility of these DPD beads at room temperature in dilute solution.<sup>23-25</sup> Moreover, the interaction parameters between the hydrophobic and hydrophilic segments were set as  $\alpha_{CE} = \alpha_{OE} = 50$ , suggesting that the hydrophobic and hydrophilic components are incompatible and phase-segregated in water.<sup>26,27</sup> To model the amphiphilic nature of multiblock copolymers, the interaction parameter between solvophobic segments and solvent were set as  $\alpha_{CW} = \alpha_{OW} = 80$ .<sup>26,27,28,29</sup> It is worth noting that the  $\chi$ -parameter between PEG and water was taken as 0.30 proposed by Groot and

Rabone,<sup>30</sup> which was fitted from experimental adsorption data by Seaki et al.<sup>31</sup> Hence, the interaction parameter between PEG and water was calculated to be  $\alpha_{EW} = 25.98$  according to equation S5.

We carried out the simulation in a cubic simulation box of size  $20 \times 20 \times 20 r_c^3$  with a periodic boundary condition to eliminate the finite size effects. The total beads were 24,000, the spring constant  $C$  was chosen as 10.0 and the time step was taken as 0.05. The simulation step was set as 100,000. All the computational works were performed using DPD program incorporated in the software Materials Studio 5.0 software (Accelrys) installed on a DELL PowerEdge SC430 server.

### **Photo-Reductive Degradation of PRSRP**

The photo-triggered self-degradation of PRSRP was first conducted in the solid phase. In brief, the polymer solution in chloroform ( $20 \text{ mg mL}^{-1}$ ) was cast on a KBr pellet and dried under vacuum at  $60^\circ\text{C}$  for 24 h. Then the pellet was irradiated with UV light at 365 nm for different times. The change in chemical structure was monitored in situ on a Nicolet iS10 spectrometer (Thermo Electron Corporation, U.S.A) from 4000 to  $500 \text{ cm}^{-1}$ . The change of pellet color was captured digitally.

To quantitatively determine the degradation kinetics, PRSRP was dissolved in *N,N*-Dimethylformamide (DMF) ( $2 \text{ mg mL}^{-1}$ ) and transferred into a quartz cuvette. Then the solution was exposed to UV irradiation (365 nm) for different times. The changes in solution overtime were monitored by UV-vis spectra measured using UV2600 spectrophotometer (Techcomp, Ltd., China).

To elucidate the photolysis mechanism, the photodegradation of PRSRP solutions

in DMSO- $d_6$  was monitored in situ by  $^1\text{H}$  NMR. Briefly, the polymer was dissolved in DMSO- $d_6$  ( $\text{mg mL}^{-1}$ ) and transferred into a quartz nuclear magnetic tube. Then the tube was treated by UV illumination for different times. At desired time intervals (0, 15, 30, 60, and 120 min), the tube was analyzed on a Bruker Avance III HD 400MHz spectrometer.

To further support the self-reduction of disulfide bond, 5 mg PRSRP was dissolved in THF and irradiated by UV light at 365 nm for 2 h. The degradation products were collected and dried for GPC analysis. MPEG monomer was also tested as a control.

### **Stimuli-Responsiveness of PRSRP Assemblies**

To study the effect of the photo-reductive degradation process of self-assembled structure, dynamic light scattering (DLS) test was first performed to monitor the vesicular size under UV irradiation. Briefly, 2 mL of polymer assemblies ( $2 \text{ mg mL}^{-1}$ ) was added into a quartz cuvette and exposed to UV light at 365 nm for 15, 30, 60, and 120 min. The solution was measured using a Zetasizer Nano ZS 90 instrument (Malvern Instruments Ltd., UK) at room temperature.

To quantitatively determine the degradation kinetics of PRSRP assemblies, the vesicular solution ( $2 \text{ mg mL}^{-1}$ ) was transferred into a quartz cuvette. Then the solution was exposed to UV irradiation (365 nm) for different times. The changes in solution overtime were monitored by a UV-Vis spectroscopy. The PRSRP assemblies before and after UV treatment was also observed on a Hitachi model H-600-4 transmission electron microscope.

### **NR Loading and Release**

Nile red (NR) was used as a hydrophobic drug model and loaded into PRSRP and PRIRP vesicles. Briefly, a solution of NR in acetone (100  $\mu\text{L}$ , 0.2  $\text{mg mL}^{-1}$ ) was gradually added dropwise to the 6 mL assembled solutions prepared from PRSRP and PRIRP (1  $\text{mg mL}^{-1}$ ) with stirring for 48 h. The solutions were centrifuged for 15 min at 3000  $\text{r min}^{-1}$  and filtered through a 0.45  $\mu\text{m}$  pore-sized syringe filter (Millipore, Carrigtwohill, Co. Cork, Ireland).

### **DOX Loading and Release**

Doxorubicin (DOX) was loaded into the PRSRP assemblies as a model hydrophobic anticancer drug. Briefly, hydrophilic DOX·HCl (10 mg) was dispersed in THF (1 mL) and desalted under ultrasonic condition in the presence of excess TEA. The solution was added dropwise into the 5 mL PRSRP assemblies with stirring. The solution was then transferred into a dialysis bag (MWCO 3500) and dialyzed against phosphate buffered saline (PBS, pH 7.4) for 3 d. The PBS solution was replaced once 3 h. Finally, the solution was centrifuged at 3000  $\text{r min}^{-1}$  for 15 min and filtered through a 0.22  $\mu\text{m}$  pore size syringe filter (Millipore, Carrigtwohill, Co. Cork, Ireland).

The release of DOX was assessed by dialysis against PBS (10 mM, pH 7.4) with or without UV light. At the desired time intervals, 2 mL of release medium was sampled and replenished with an equal volume of fresh medium. Release experiments were performed in triplicate. The amount of released DOX was determined by a UV-Vis spectrometer (UV-2600, Shanghai Techcomp Instrument Co., Ltd, Shanghai, China).

Since the release of DOX is too fast to attain a favorable sink condition, the drugs precipitate in the dialysis bag. To visually demonstrate the ultrafast release of DOX, the

DOX-loaded PRSRP vesicles were added into vials and subjected to UV irradiation (365 nm) or GSH treatment (10 mM). The change in solution was captured digitally.

### **Forster Resonance Energy Transfer (FRET) Measurement**

30  $\mu$ L of triethylamine (TEA) was added into 1 mL of DOX (1 mg mL<sup>-1</sup>) and 3,3'-diethylthiadicarbocyanine iodide (Cy5) (2 mg mL<sup>-1</sup>) solution in Dichloromethane (DCM), and sonicated at room temperature for 120 min. The DCM was dried by a flow of argon and the bottle was added with 5 mL of PRSRP dispersions in water. After incubation in an ultrasound bath for 2 h, the solution was dialyzed against deionized water for 24 h (MWCO 3500), then centrifuged for 10 min at 3500 r min<sup>-1</sup>, and through a 0.22  $\mu$ m pore size syringe filter (Millipore, Carrigtwohill, Co. Cork, Ireland). The DOX and Cy5 coloaded PRSRP assemblies were irradiated with UV light (365 nm) for 4 min, or treated with 10 mM dithiothreitol (DTT). The change of fluorescence spectra over time was monitored using an F-4600 FL spectrophotometer (Hitachi, Ltd., Japan). The excitation wavelength was 480 nm and the slit width was 5.0 nm. The ratio of fluorescence intensity at 598 nm to that at 676 nm was normalized and plotted over time.

### **Cell Internalization**

MCF-7 breast cancer cells were cultured in a petri dish to about 80% full, digested with trypsin, then transferred to a 15 mL centrifuge tube, and centrifuged at 1000 r min<sup>-1</sup> for 3 min to remove the upper liquid, then diluted with high-sugar medium, inoculated into a 6-well plate (built-in cell slide) at a density of  $1 \times 10^5$  cells mL<sup>-1</sup>. The cells were cultured in a high sugar medium containing a double antibody (1%) and fetal bovine



serum (10%) at 37 °C under 5% CO<sub>2</sub>. After 24 h, fluorescent-labeled PRSRP assemblies were added and pre-incubated for 1 h. Then the cells were incubated for additional 3 h without or with UV irradiation (365 nm) for 4 min before incubation. The medium was removed, washed gently for three times with PBS. Then the cells were fixed with 4% formaldehyde for 30 min and stained with DAPI for 10 min. At last, the coverslips were mounted with 50% glycerol solution and observed on a confocal laser scanning microscope (CLSM, Olympus FV1000, Japan).

### **Endocytosis mechanism**

To evaluate the endocytosis mechanism of PRSRP micelles, MCF-7 cells were seeded in a six-well plate (a coverslip was placed in every well ahead of use) at a density of  $1 \times 10^5$  cells per well and cultured overnight. Then the cells were pre-incubated with different inhibitors: methyl- $\beta$ -cyclodextrin (2.5 mM), chlorpromazine ( $10 \mu\text{g mL}^{-1}$ ), colchicine ( $8 \mu\text{g mL}^{-1}$ ), genistein ( $50 \mu\text{g mL}^{-1}$ ) for 2 h at 37 °C. Meanwhile, another two groups of cells were pre-incubated without inhibitor at 4 °C and 37 °C for 2 h. Cells without pretreatment were set as control. Then DOX@PRSRP micelles were added into the plate with a consistent drug concentration of  $10 \mu\text{g mL}^{-1}$  and incubated at 37 °C or 4 °C for 4 h. Finally, the cells were washed, digested, centrifuged and resuspended for flow cytometer measurement. For CLSM observation, the cells were HeLa cells were cultured in a six-well plate (a coverslip was placed in every well before use) and treated as described above. The medium was removed, washed gently for three times with PBS. Then the cells were fixed with 4% formaldehyde for 30 min and stained with DAPI for 10 min. At last, the coverslips were mounted with 50% glycerol solution and observed

on a confocal laser scanning microscope (CLSM, Olympus FV1000, Japan).

### MTT Assay

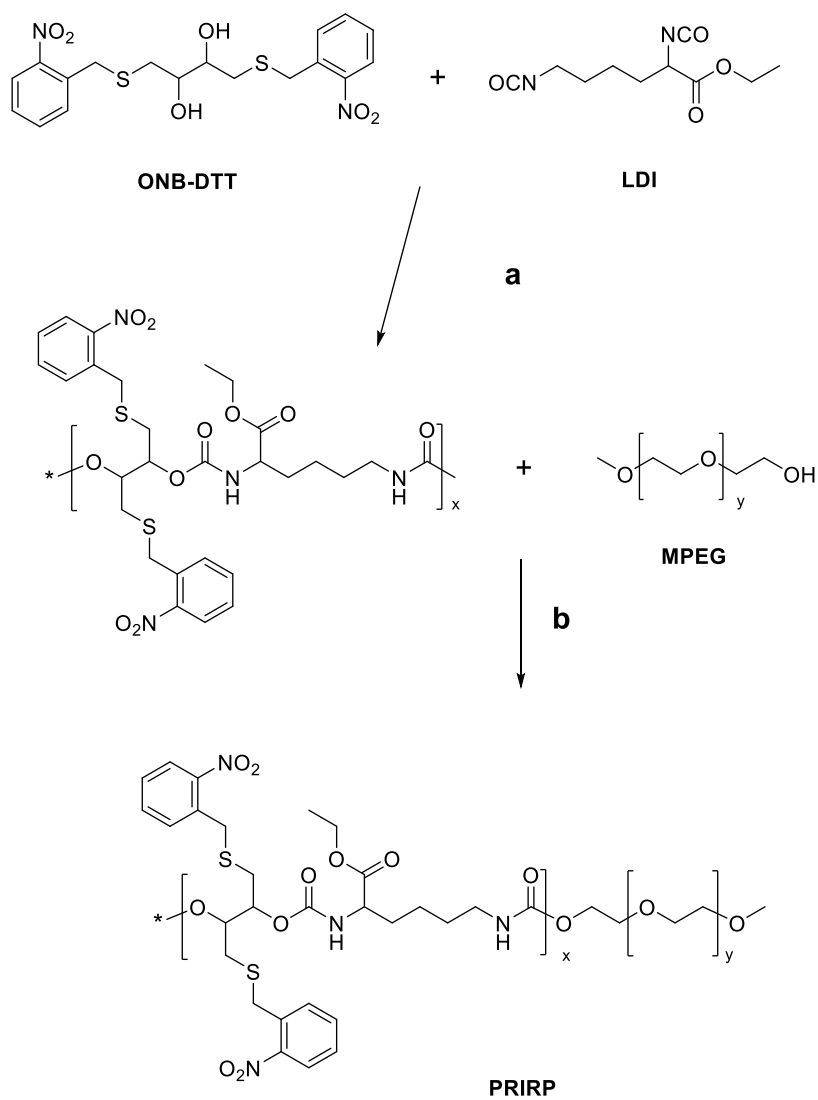
MTT assay was used to determine the toxicity of drug-loaded polymer assemblies. Briefly, MCF-7 cells were seeded in a 96-well plate at a density of  $5 \times 10^4$  cell per well (100  $\mu$ L per well). The cells were incubated for 24 h in a humidified atmosphere of 5% CO<sub>2</sub> at 37 °C (Sanyo Incubator, MCO-18AIC, Japan). The culture media was removed and replaced with 100  $\mu$ L media containing DOX@PRSRP with different concentrations. Free DOX solution with an equal DOX concentration was set as a positive control, and blank culture medium was used as a negative control. For photo-responsive group, the wells containing DOX@PRSRP were exposed to UV light (365 nm) for 4 min. After 48 h of incubation, 20  $\mu$ L of MTT solution (5 mg mL<sup>-1</sup>) was added to each well and incubation was continued for 4 h in the incubator. The upper liquid was carefully aspirated, and the wells were added with 200  $\mu$ L of dimethyl sulfoxide (DMSO). The mixture was shaken for 10 min to completely dissolve insoluble formazan crystals, and the absorbance OD value of each well was measured at a wavelength of 490 nm by a microplate reader (DNM-9602, Nanjing Perlove Medical Equipment Co., Ltd., China). Relative cell survival rate was calculated according to the following equation: cell viability =  $A_{\text{sample}} / A_{\text{control}} \times 100\%$ , where  $A_{\text{sample}}$  and  $A_{\text{control}}$  indicate the OD values of polymeric formulations and negative control, respectively. To investigate the cytocompatibility of PRSRP, the survival rates MCF-7 cells incubated with drug-free PRSRP assemblies and their degradation products were also tested by MTT assay as described above.

## **Statistical Analysis**

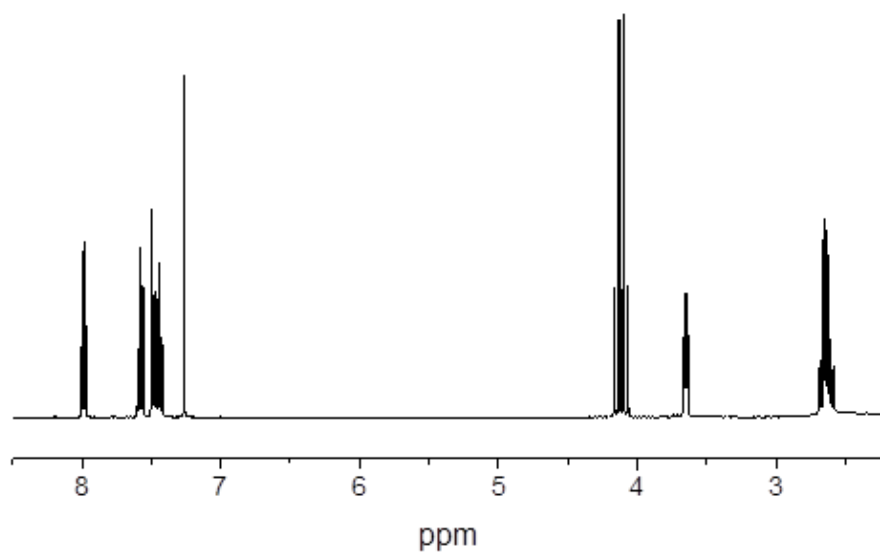
The quantitative data were expressed as means  $\pm$  standard deviations (SD). Statistical analysis was performed with a Statistical Package for the Social Sciences (IBM SPSS Statistics software, Version 19, IBM, New York, USA). Student's t-test or one-way analysis of variance (ANOVA) was carried out to determine the statistical significance within the data at 95% confidence levels ( $P < 0.05$ ).

## Supporting Figures and Tables

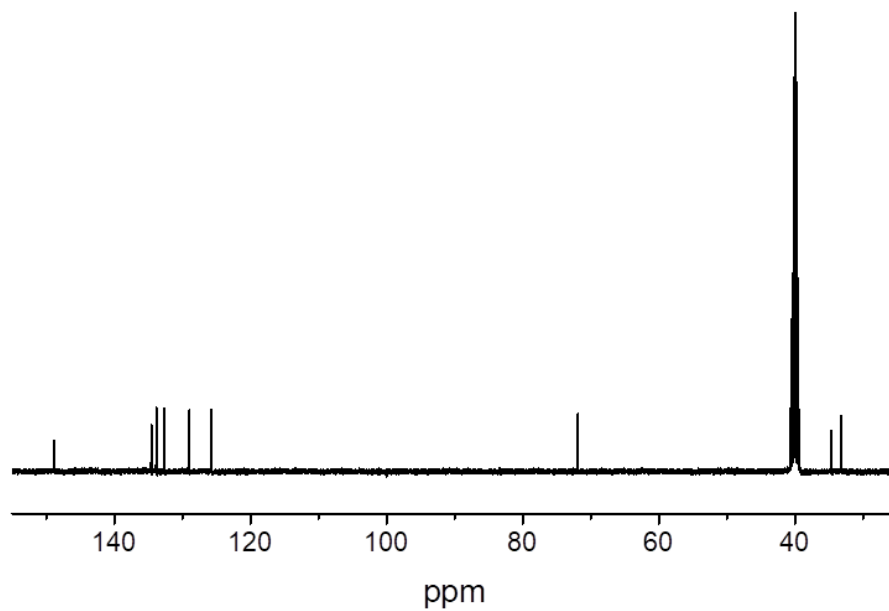
**Scheme S1.** Synthesis of photo-responsive irreducible polymer.<sup>a</sup>



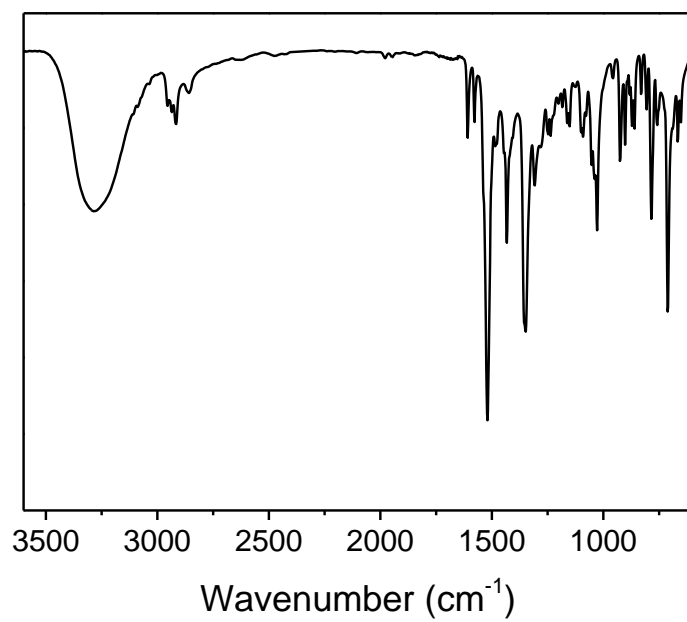
<sup>a</sup> Reagents and conditions: (a) THF, 60 °C, 12 h. (b) THF, 80 °C, 24 h (81.4% yield).



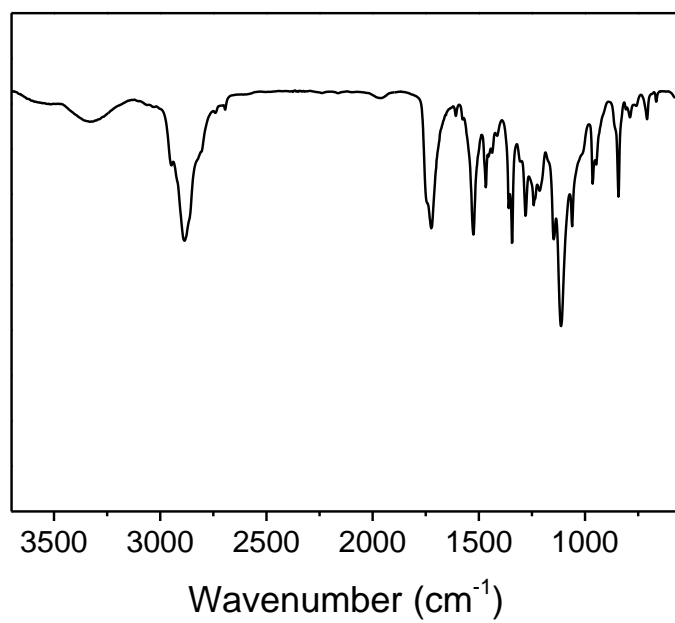
**Figure S1.** 400 MHz <sup>1</sup>H NMR spectrum of ONB-DTT in CDCl<sub>3</sub>.



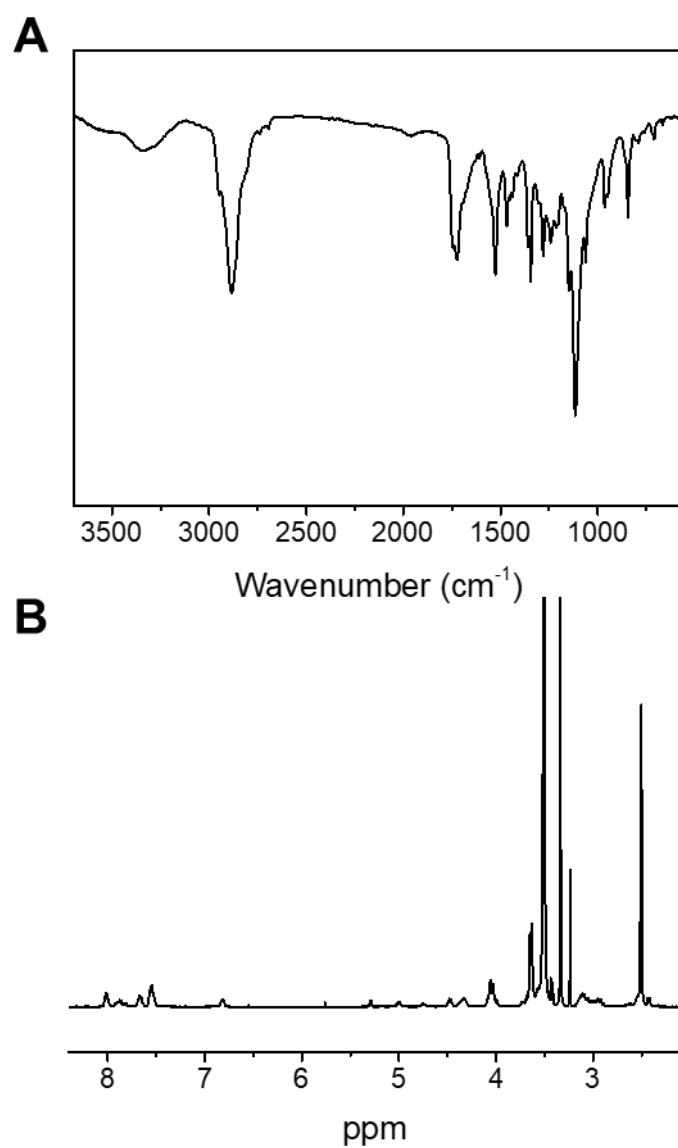
**Figure S2.** 600 MHz <sup>13</sup>C NMR spectrum of ONB-DTT in DMSO-*d*<sub>6</sub>.



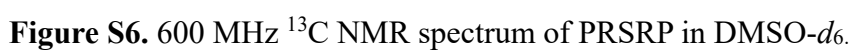
**Figure S3.** FTIR spectrum of ONB-DTT.



**Figure S4.** FTIR spectrum of PRSRP.



**Figure S5.** FTIR spectrum (A) and 400 MHz  $^1\text{H}$  NMR spectrum (B) of PRSRP-O.





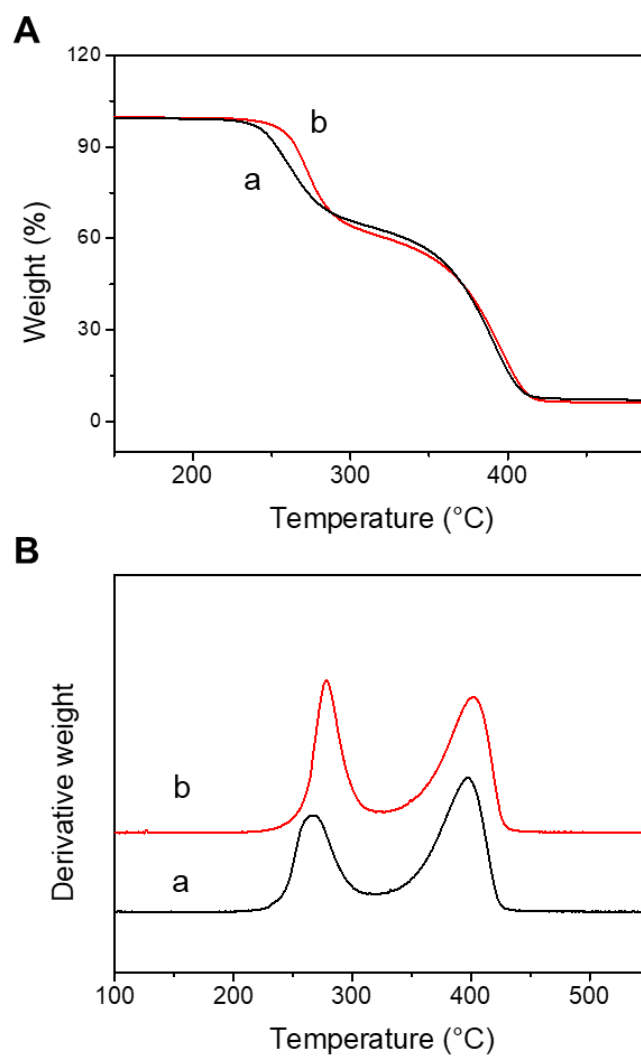


**Figure S7.** (A) TGA curves and (B) DTG curves of photo-responsive self-reducible polymers: (a) PRSRP-O and (b) PRSRP.

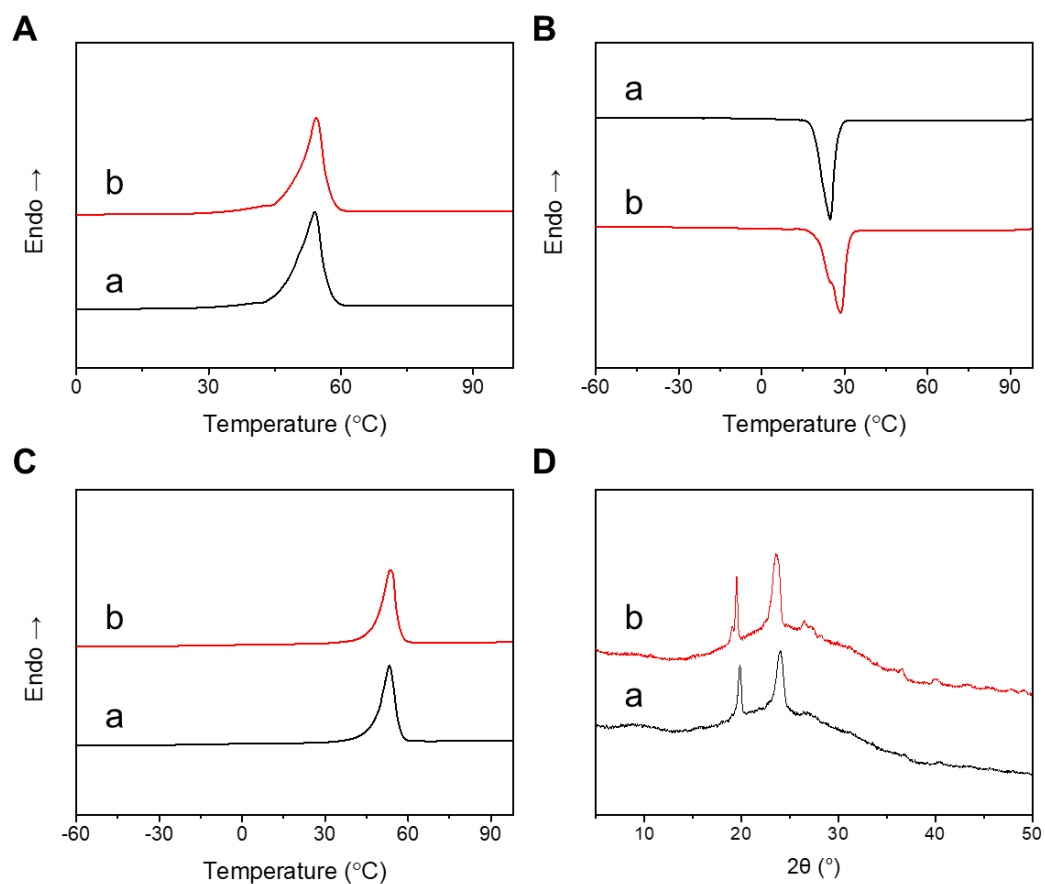


**Figure S8.** DSC curves of PRSRP-O (a) and PRSRP (b). (A) First heating traces from 0 to 100 °C. (B) The cooling traces from 100 to -90 °C. (C) The second heating traces from -90 to 100 °C. (D) XRD patterns of PRSRP-O (a) and PRSRP (b).

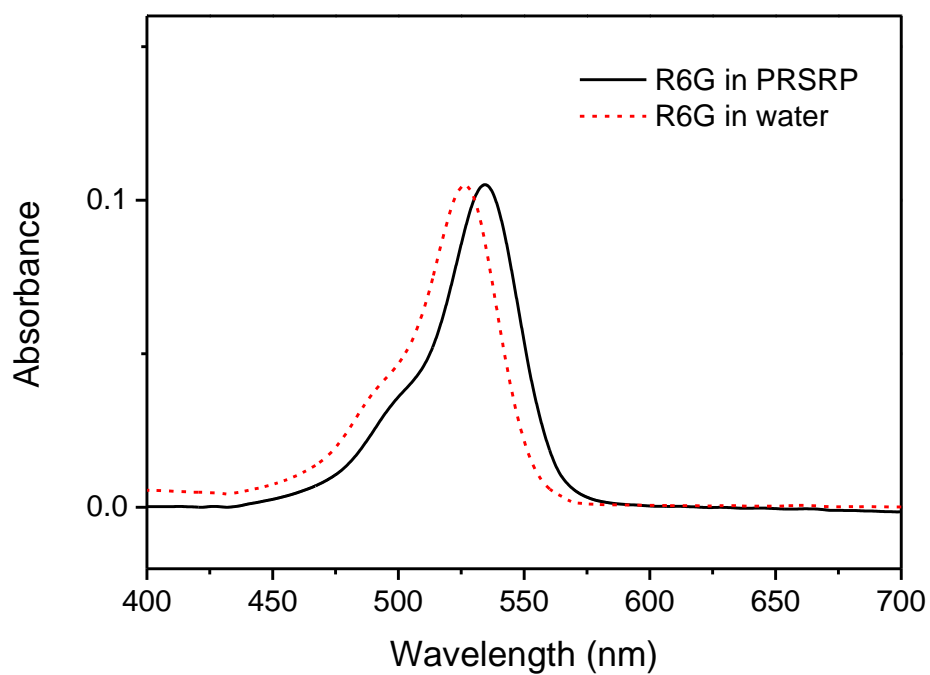


**Figure S9.** UV-Vis spectrum of R6G solution in water and that in the presence of PRSRP assemblies. The concentration of free R6G solution in water was adjusted so that the absorbance matched that of R6G in assembled solutions.

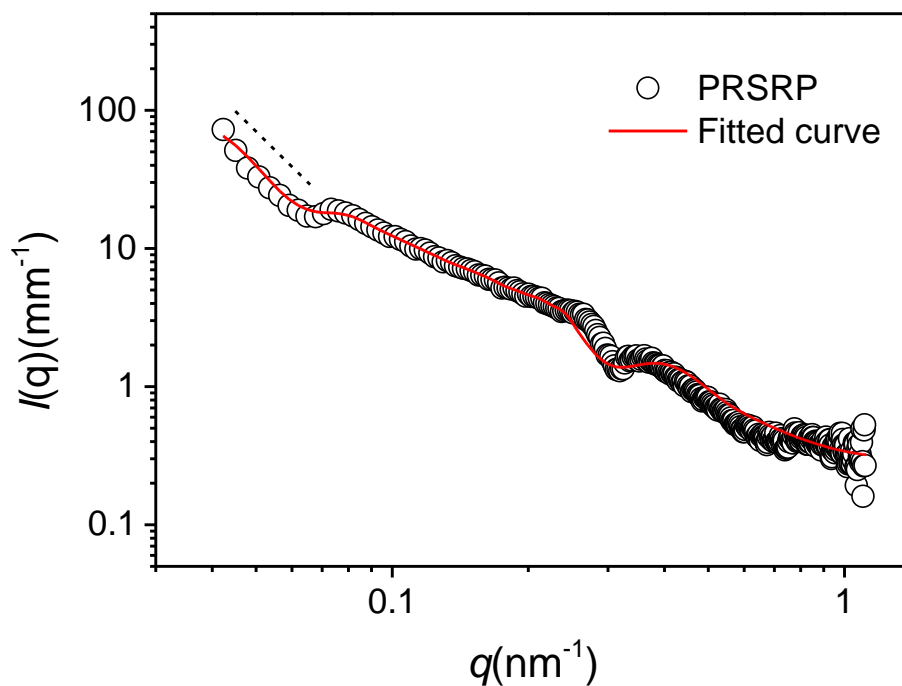


**Figure S10.** SAXS scattering data of photo-responsive self-reducible polymer in the low  $q$  region. The red solid line represents a fit of the data, and the dash line shows the gradient of the curve.

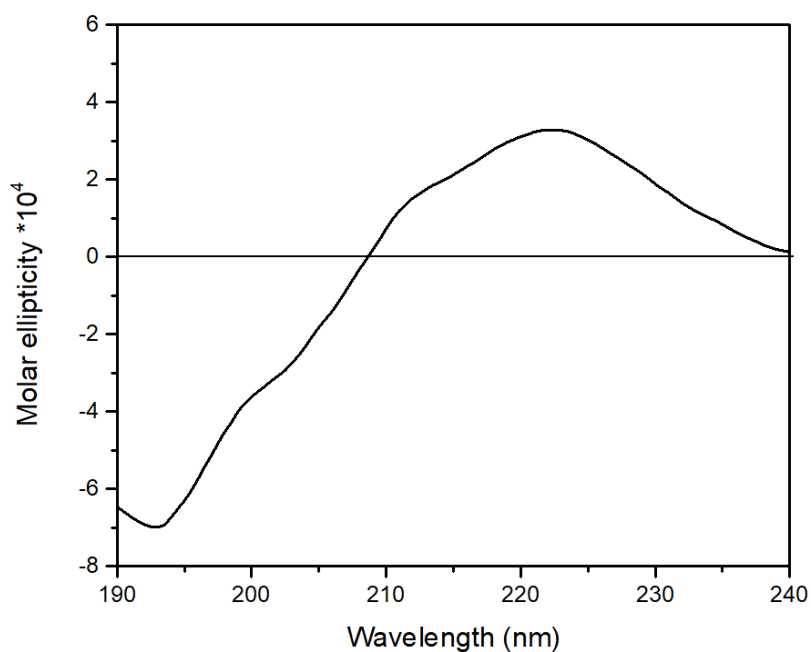


**Figure S11.** CD spectrum of photo-responsive self-reducible polymer.

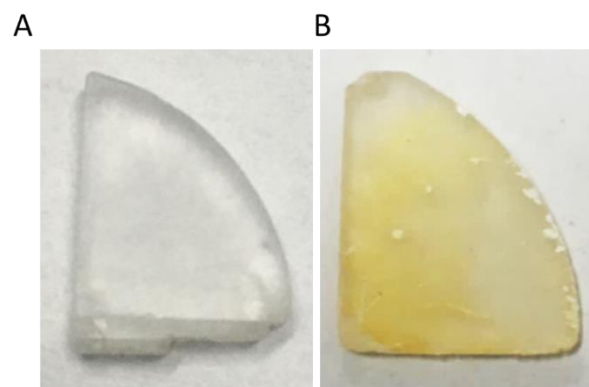


**Figure S12.** PRSRP cast on a KBr pellet before (A) and after (B) exposure to UV light (365 nm) for 2 h.

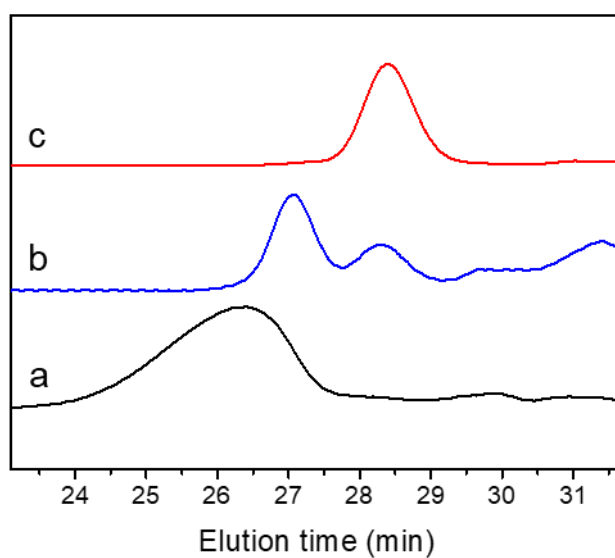


**Figure S13.** GPC curves of PRSRP before (a) and after (b) UV irradiation for 2 h, taking MPEG monomer (c) as a control.

2019014371-THF #1601-1627 RT: 14.48-14.72 AV: 27 SB: 109 13.03-14.01 NL: 1.00E5  
T: + c ESI Q1MS [120.000-1500.000]

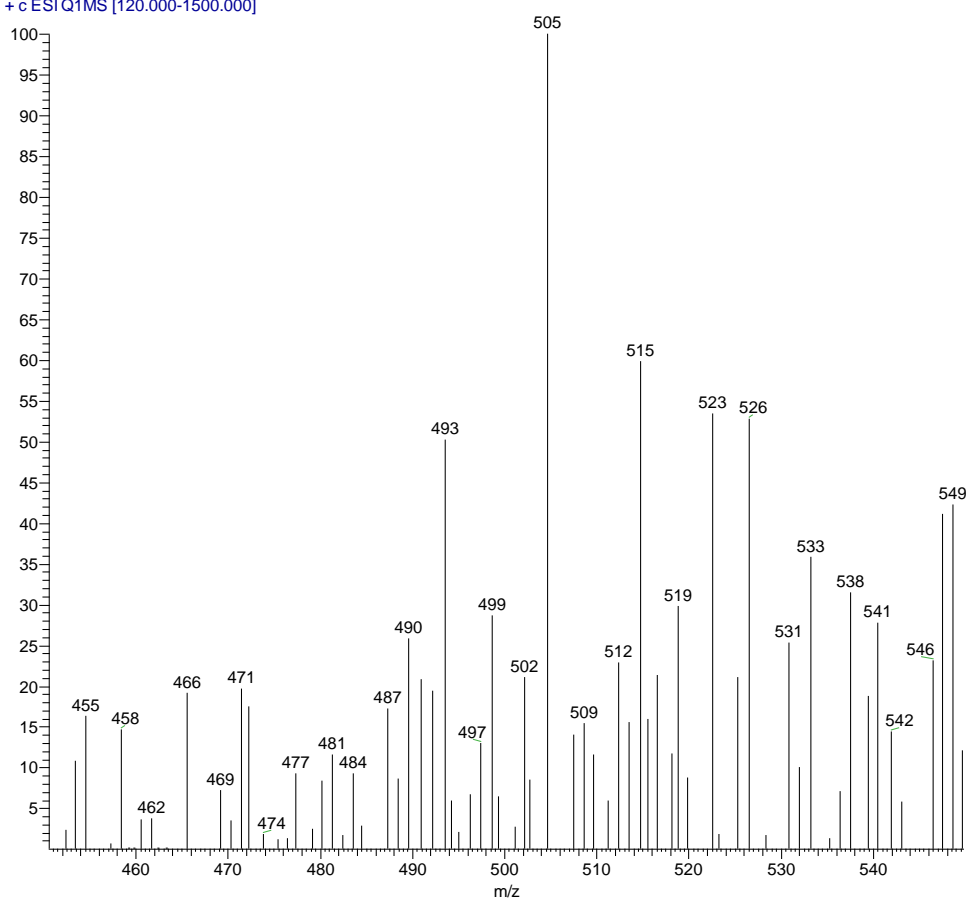


**Figure S14.** MS spectra of photo-reductive degradation products of PRSRP. The polymer solution was irradiated with UV light (365 nm) for 2 h and subjected to MS analysis. As expected, a peak observed at  $m/z = 497$  can be assigned to a small molecular fragment, di-*N*-acetyl-L-cysteine methyl ester-modified 1,2-dithiane derivative ( $[M+Na]^+$ , Figure 4). Moreover, the signals corresponding to the dimer of the product was also detected (474 for  $[2M+2H]^{2+}$ ; 493 for  $[2M+H+K]^{2+}$ ; 505 for  $[2M+Na+K]^{2+}$ ; 512 for  $[2M+2K]^{2+}$ ).

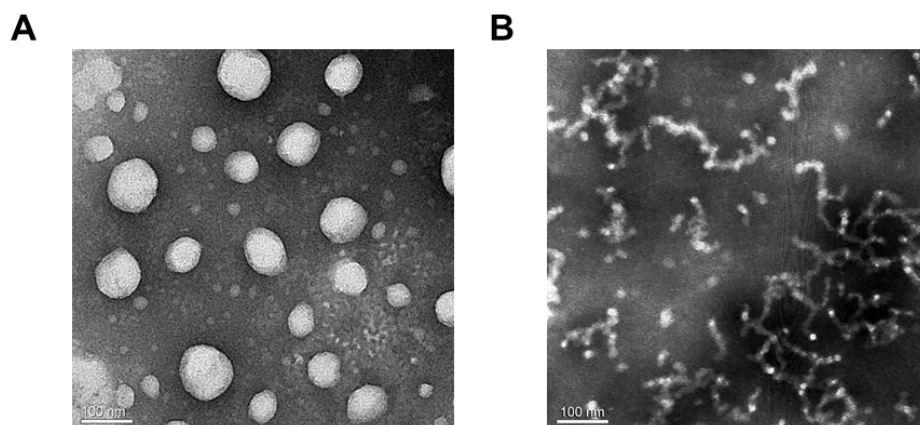


**Figure S15.** TEM micrographs of PRSRP assemblies before (A) and after 2h of UV irradiation (B). The bars are 100 nm.

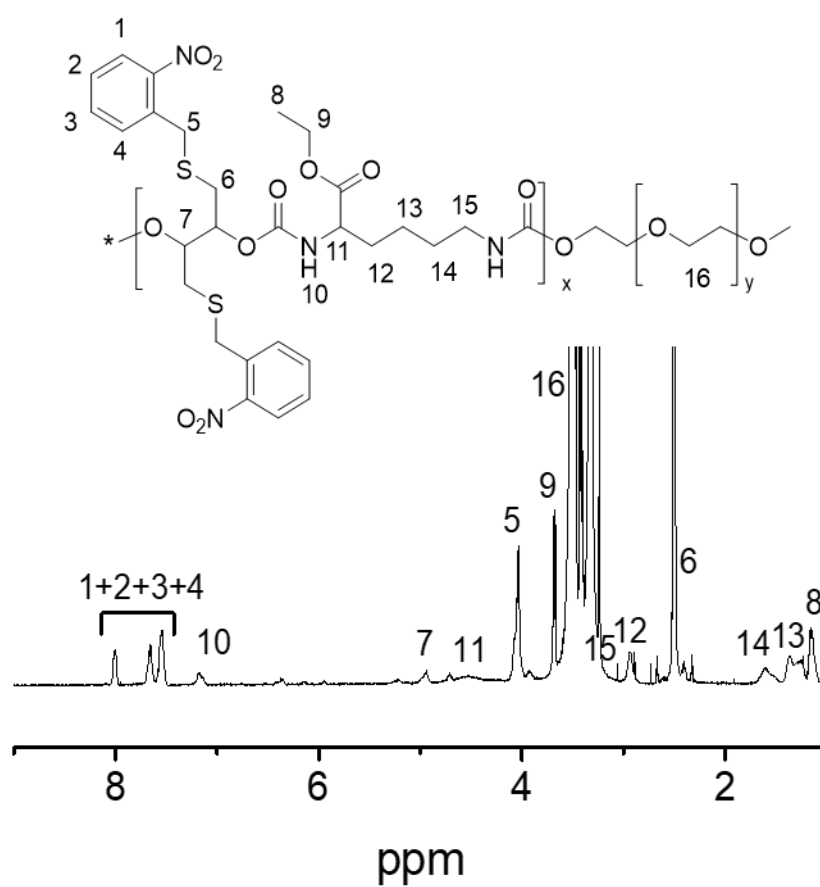


**Figure S16.** 400 MHz  $^1\text{H}$  NMR spectra of PRIRP in  $\text{DMSO-}d_6$ .

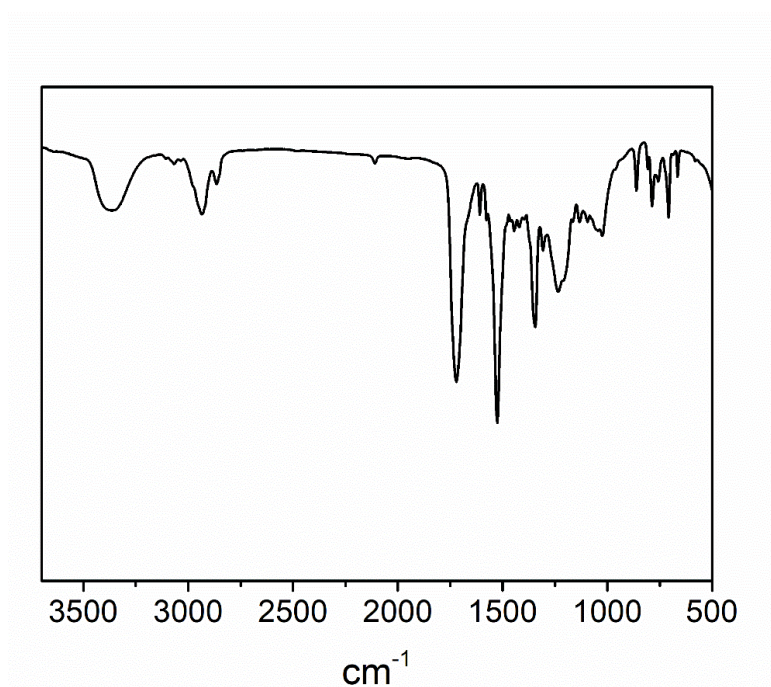


**Figure S17.** FTIR spectrum of PRIRP

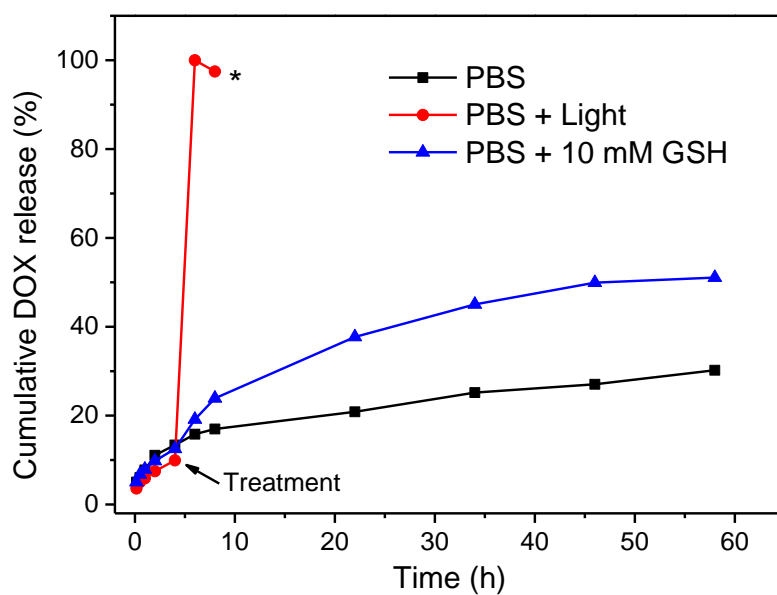


**Figure S18.** Cumulative release profiles of DOX from PRSRP assemblies in PBS solutions with different treatments. The arrow shows the onset of UV irradiation or GSH treatments. The asterisk indicates that the drugs precipitate in the dialysis bag.



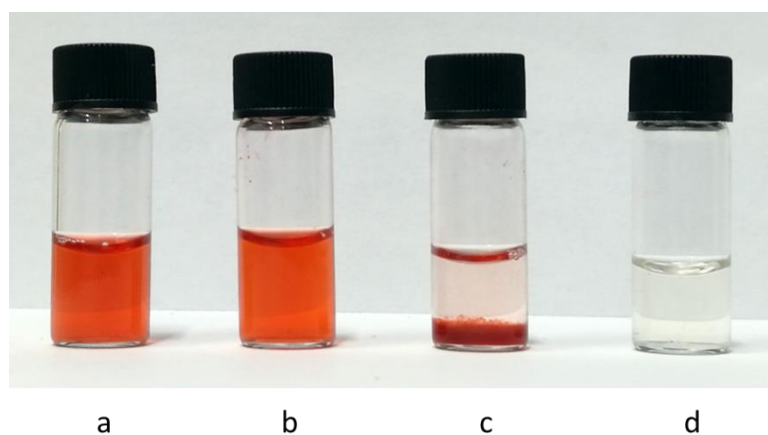


**Figure S19.** Photographs of DOX-loaded PRSRP assemblies without (a) and with GSH treatment (b) and UV irradiation (c). (d) shows drug-free assemblies.

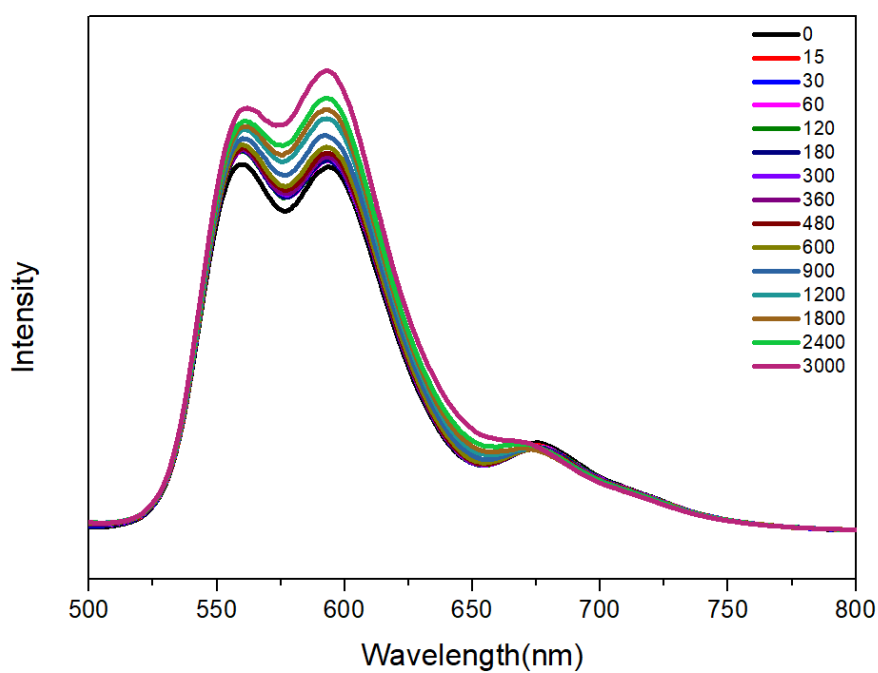


**Figure S20.** Typical fluorescence emission spectra ( $\lambda_{\text{ex}} = 480 \text{ nm}$ ) of PRSRP assemblies loading with DOX and Cy5 after addition of DTT for different times.

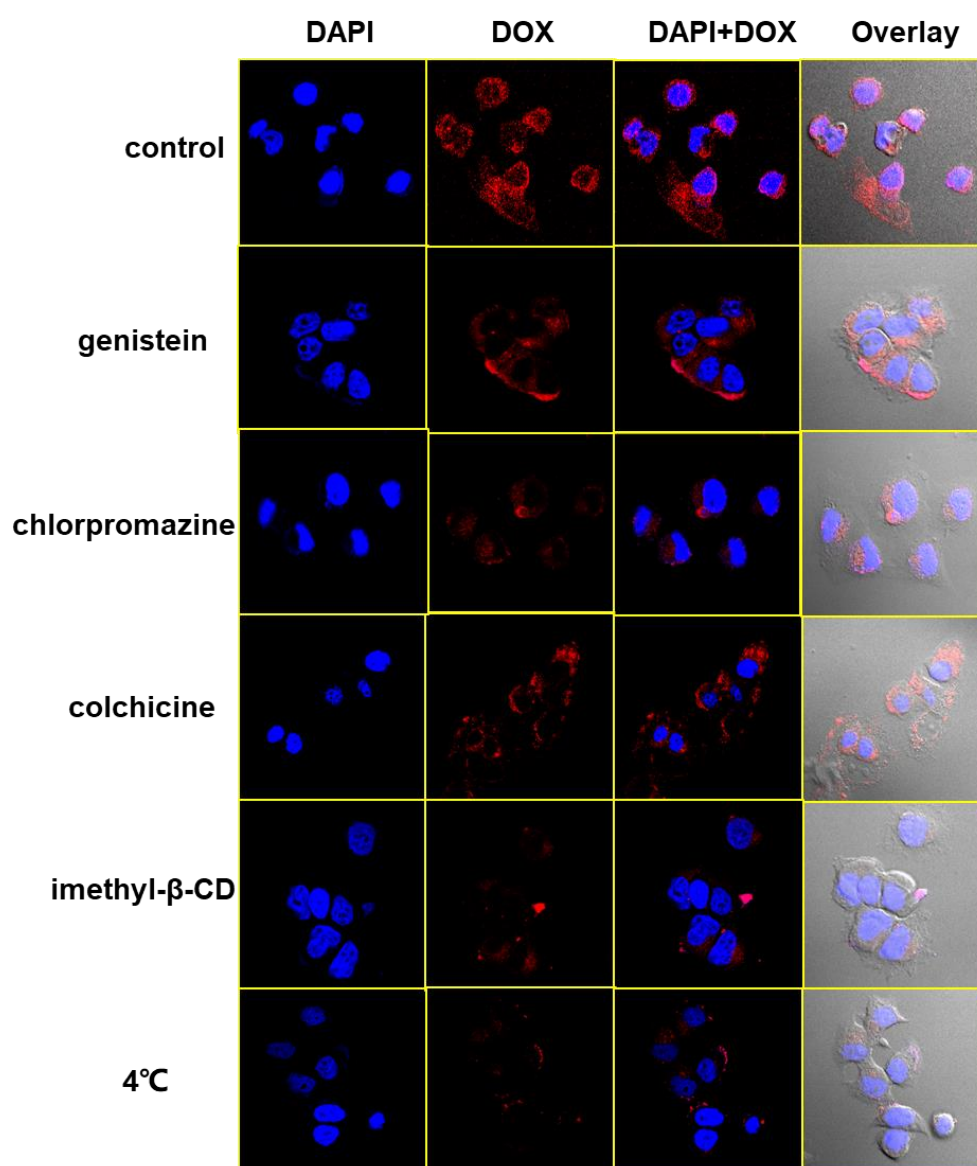


**Figure S21.** CLSM images of MCF-7 cancer cells incubated with DOX@PRSRP for 4 h at 4 °C and at 37 °C in the presence of different inhibitors. Nuclei of cells were stained with DAPI.

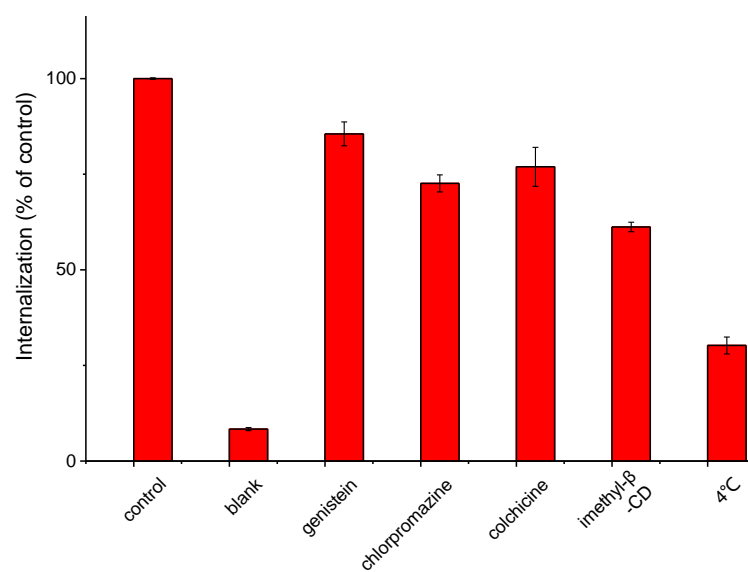


**Figure S22.** Flow cytometry of MCF-7 cancer cells incubated with DOX@PRSRP for 4 h at 4 °C and at 37 °C in the presence of different inhibitors.

**Table S1.** Synthesis and molecular composition of photo-responsive self-reducible and irreducible polymers.

Samples <sup>a</sup>	$M_n$ <sup>b</sup> (g mol <sup>-1</sup> )	$M_w$ <sup>b</sup> (g mol <sup>-1</sup> )	PDI <sup>b</sup>
PRSRP	12900	13700	1.16
PRSRP-O	5200	5580	1.07
PRIRP	12483	17358	1.39

<sup>a</sup> Photo-responsive polymers with different molecular weight and chemical structures.

PRSRP and PRSRP-O represent photo-responsive self-reducible polymer and oligomer.

PRIRP represents photo-responsive irreducible polymer prepared using LDI as a coupling agent instead of CDI.

<sup>c</sup> Molecular weights and molecular weight distributions determined by GPC.

## Supporting references

- 1 Liu. H, Wang. R, Wei. J, Cheng. C, Zheng. Y, Pan. Y, He. X, Ding. M, Tan. H and Fu. Q, *J. Am. Chem. Soc.* **2018**, 140, 6604.
- 2 Feng. Z, Wang. H, Wang. S, Zhang. Q, Zhang. X, Rodal. A. A and Xu. B, *J. Am. Chem. Soc.* **2018**, 140, 9566.
- 3 Liu. T, Diemann. E and Müller. A, *J. Chem. Educ.* **2007**, 84, 526.
- 4 Li. H, Wang. R, Hong. Y. I, Liang. Z, Shen. Y, Nishiyama. Y, Miyoshi. T and Liu. T, *Eur. Respir. J.* **2019**, 25, 5803.
- 5 Yin. P, Wu. B, Mamontov. E, Daemen. L. L, Cheng. Y, Li. T, Seifert. S, Hong. K, Bonnesen. P. V and Keum. J. K, *J Am Chem Soc.* **2016**, 138, 2638.
- 6 Mable. C. J, Derry. M. J, Thompson. K. L, Fielding. L. A, Mykhaylyk. O. O and Armes. S. P, *Macromolecules.* **2017**, 50, 4465.
- 7 Folkertsma. L, Zhang. K, Czakkel. O, de Boer. H. L, Hempenius. M. A, van den Berg. A, Odijk. M and Vancso. G. J, *Macromolecules.* **2016**, 50, 296.
- 8 Hordyjewicz-Baran. Z, You. L, Smarsly. B, Sigel. R, and Schlaad. H, *Macromolecules.* **2007**, 40, 3901.
- 9 Zhou. Y and Yan. D, *Angew. Chem. Int. Ed.* **2004**, 43, 4896.
- 10 Cockram. A. A, Neal. T. J, Derry. M. J, Mykhaylyk. O. O, Williams. N. S. J, Murray. M. W, Emmett. S. N and Armes. S. P, *Macromolecules.* **2017**, 50, 796.
- 11 Bang. J, Jain. S, Li. Z, Lodge. T. P, Pedersen. J. S, Kesselman. E and Talmon. Y, *Macromolecules.* **2006**, 39, 1199.
- 12 Kukula. H, Schlaad. H, Antonietti. M and Förster. S, *J. Am. Chem. Soc.* **2002**, 124, 1658.
- 13 Truong. N. P, Zhang. C, Nguyen. T. A. H, Anastasaki. A, Schulze. M. W, Quinn. J. F, Whittaker. A. K, Hawker. C. J, Whittaker. M. R and Davis. T. P, *ACS Macro Lett.* **2018**, 7, 159.
- 14 Peng. S, Guo. Q, Hughes. T. C and Hartley. P. G, *Macromolecules.* **2011**, 44, 3007.
- 15 Lund. R, Willner. L, Richter. D, Lindner. P and Narayanan. T, *ACS Macro Lett.*

- 2013**, 2, 1082.
- 16 Zhou. Z, Li. Z, Ren. Y, Hillmyer. M. A and Lodge. T. P, *J. Am. Chem. Soc.* **2003**, 125, 10182.
  - 17 Derry. M. J, Mykhaylyk. O. O and Armes. S. P, *Angew. Chem. Int. Ed.* **2017**, 56, 1746.
  - 18 Kučerka. N, Pencser. J, Sachs. J. N, Nagle. J. F and Katsaras. J, *Langmuir*. **2007**, 23, 1292.
  - 19 Groot. R. D and Warren, P. B, *J. Phys. Chem.* **1997**, 107, 4423.
  - 20 Li. X, Deng. M, Liu. Y and Liang. H, *J. Phys. Chem. B.* **2008**, 112, 14762.
  - 21 Li. X, Liu. Y, Wang. L, Deng. M and Liang. H, *Phys. Chem. Chem. Phys.* **2009**, 11, 4051.
  - 22 Liu. D and Zhong. C, *Polymer*. **2008**, 49, 1407.
  - 23 Tan. H, Yu. C, Lu. Z, Zhou. Y and Yan. D, *Soft Matter*. **2017**, 13, 6178.
  - 24 Ma. S, Xiao. M and Wang. R, *Langmuir*. **2013**, 29, 16010.
  - 25 Li. X, *Soft Matter*. **2013**, 9, 11663.
  - 26 Lin. Y.-L, Chang. H.-Y, Sheng. Y.-J and Tsao. H.-K, *Soft Matter*. **2014**, 10, 1500.
  - 27 Lin. Y.-L, Chang. H.-Y, Sheng. Y.-J and Tsao. H.-K, *Soft Matter*. **2014**, 10, 1840.
  - 28 Lin. Y.-L, Chang. H.-Y, Sheng. Y.-J and Tsao. H.-K, *Soft Matter*. **2013**, 9, 4802.
  - 29 Arai. N, Yasuoka. K and Zeng. X. C, *ACS Nano*. **2016**, 10, 8026.
  - 30 Groot. R. D and Rabone. K, *Biophys. J.* **2001**, 81, 725.
  - 31 Saeki. S, Kuwahara. N, Nakata. M and Kaneko. M, *Polymer*. **1976**, 17, 685.